



Contents lists available at ScienceDirect

Journal of Hydrology

journal homepage: www.elsevier.com/locate/jhydrol

Hierarchical modeling of a groundwater remediation capture system



Hua-Sheng Liao, Prasanna V. Sampath, Zachary K. Curtis, Shu-Guang Li*

Dept. of Civil & Environmental Engineering, Michigan State University, East Lansing, MI 48824, United States

ARTICLE INFO

Article history:

Received 4 March 2015

Accepted 24 April 2015

Available online 8 May 2015

This manuscript was handled by Corrado Corradini, Editor-in-Chief, with the assistance of Stephen Worthington, Associate Editor

Keywords:

Multi-scale modeling
Pump-and-treat system
Particle tracking
Parameter estimation

SUMMARY

In this paper, we present a real-world demonstration of a generalized hierarchical approach for modeling complex groundwater systems, the hierarchical patch dynamics paradigm (HPDP). In particular, we illustrate how the HPDP approach enables flexible and efficient simulation of a complex contaminant capture system at one of the largest groundwater pump-and-treat remediation operations in Michigan. The groundwater flow system at the site exhibits a multi-scale pattern that is difficult to simulate using standard modeling tools because of the complex interaction between ambient hydrologic stresses and on-site remediation operations. The hierarchical modeling system was calibrated to water level measurements collected from 208 monitoring wells located both on-site and in its immediate proximity and flux measurements from 6 trenches on-site. Systematic hierarchical simulations, including forward and reverse particle tracking as well as integrated water budget analyses, were performed to study the on-going remediation. The hierarchical modeling results show that some contamination leaked off-site because of small-scale inefficiencies in the design of the remediation system. Thus, the HPDP approach provides an opportunity to analyze complex hydrological field environments in a pragmatic, time-efficient manner.

Published by Elsevier B.V.

1. Introduction

In many groundwater systems, complex configurations of stresses and the hydrogeological environment leads to multi-scale variability of the flow field in space and time. Characterizing such complexity is critical for evaluation of groundwater management, especially pollution control and remediation (Afshari et al., 2008). In such circumstances numerical models are used to simulate the groundwater system and predict solute transport, using many discrete cells to represent the aquifer system and the head values at model nodes to estimate the velocity field. Generally, real-world problems extend over large geographic areas, requiring that the model utilizes numerical cells with large spatial dimensions and large time-steps relative to the small-scale variability (e.g., injection/extraction wells with rapid head variability in space and time). This is necessary to avoid (a) computational costs that are prohibitively expensive or (b) ill-posed matrices that are result of using a single numerical representation of a complex system (Li et al., 2006). The resulting simulated heads from a regional model in close proximity to point sources or sinks are generally bad approximations, despite correct predictions of head further from the well (Anderson and Woessner, 1992). Alternatively, if one

simulates local- or site-scale models independently, they may misrepresent the regional processes and thus lose the ability to accurately analyze the impact of regional variations (e.g., seasonal irrigation) on the groundwater management strategies.

Modeling across multiple scales while ensuring computational practicality and absence of numerical problems has thus become an important issue in groundwater modeling over the past few decades. The challenge of multi-scale modeling has been addressed in several different ways, including (1) local grid refinement (Fung, 1992; Gable et al., 1996; Heinemann et al., 1983); (2) local analytical correction (Prickett, 1967; Peaceman 1978; Pritchett and Garg, 1980); (3) local nested numerical correction (Ward et al., 1987; Efendiev et al., 2000; Mehl and Hill, 2002); (4) the hierarchical patch dynamics paradigm (HPDP), more recently developed and verified with a handful of synthetic examples (Li et al., 2006; Afshari et al., 2008). In this study, we present one of the first field applications of HPDP by simulating multi-scale flow and transport dynamics associated with an extensive pump-and-treat remediation operation. First, we review the advantages and disadvantages of the various multi-scale approaches.

1.1. Local grid refinement

Local grid refinement is the process of subdividing relatively large-sized cells in a numerical model into cells of smaller spatial

* Corresponding author. Tel.: +1 (517) 432 1929; fax: +1 (517) 355 0250.

E-mail address: lishug@egr.msu.edu (S.-G. Li).

dimensions in the areas of interest. This results in a more accurate estimation of hydraulic gradients at the well-scale (Fung, 1992; Gable et al., 1996; Heinemann et al., 1983; Matott et al., 2006; Sutradhar and Paulino, 2004). Applications for simple or small-scale problems provides solutions quickly while maintaining consistency between the regional and local areas around while. However, for large-scale regional groundwater models, where there may be a significant increase in the number of nodes (e.g., millions rather than thousands), the cost of computation increases exponentially and the process can become very expensive in terms of time and computer resources required.

1.2. Local analytical correction

An approach for representing detailed well dynamics in a regional model has involves a local analytical correction within the cell containing the well based on the steady-state Thiem equation (Thiem, 1906; Anderson and Woessner, 1992). Trescott et al. (1976) systematically evaluated the performance of local analytical correction and showed that corrected drawdown is approximately applicable if the following assumptions are satisfied: (1) flow to the well is within a square finite-difference cell and can be described by a steady-state equation with no source term except for the well discharge, (2) the aquifer is isotropic and homogenous in the well cell, (3) only one well, located at the cell center, is in the well cell, and (4) the well fully penetrates the aquifer. Pritchett and Garg (1980) provided formulas for analytical correction for grid cell geometries other than square. Our own empirical experience shows that local analytical correction can lead to problematic flow patterns around the wells although the corrected drawdown is reasonably accurate.

1.3. Local numerical correction

Nested grid modeling, or “local numerical correction”, is a more general approach for modeling well-scale processes within a regional model. This approach utilizes grid-dependent information from the regional model to construct a separate model with finer grid spacing around the area of interest to resolve more details (Ward et al., 1987; Efendiev et al., 2000; Mehl and Hill, 2002). Often called the “submodel”, “Local model”, or “Patch model”, the finer grid model derives its initial and boundary conditions from the parent model (Townley and Wilson, 1980; Ward et al., 1987; Buxton and Reilly, 1986). The boundary conditions can be either interpolated heads or fluxes, constraining the finer grid to then perform as an independent model. Thus, the original problem of solving a very large matrix system (encountered with local grid refinement) is avoided by converting the problem to one that requires solving a multitude of much smaller matrix systems.

In nested grid modeling, the interaction between the parent and local models depends on the offline analysis and processing of model modifications or simulation results from the parent model to obtain the boundary and starting conditions for the local model. This represents a major bottleneck in implementing this approach because making modifications to models or processing simulation results for use in different scales can be very time consuming. This is especially the case for transient flow problems and flow simulations coupled with solute transport (Li et al., 2006). When offline conceptual changes must be made iteratively in more than one model, the effort involved may become impractical (Li and Liu, 2006a,b). Additionally, a feedback loop is needed to account for potential significant two-way interactions between the parent and its nested submodels. Therefore, applications of the nested grid approach are often implemented with little flexibility to just a few sub-models.

1.4. The hierarchical patch dynamics paradigm

The hierarchical patch modeling approach was introduced by Li et al. (2006) to overcome the limitations of local numerical correction through the use of dynamic coupling between the parent and submodels. All patch models are integrated at the end of each time step during a simulation so that any changes or results (e.g., boundary conditions) to or from the parent model automatically propagate to all submodels in the model hierarchy. This is made possible by the fact that HPDP is supported by the Interactive Groundwater modeling environment (Li and Liu, 2006a,b). This environment enables the creation of submodels without the need for offline-post processing; the modeler can insert interactively and recursively a hierarchy of submodels throughout the simulation process. The results are continually displayed at the end of each time step, allowing for conceptual changes and analysis without forcing the modeler to wait until the entire simulation is complete.

Li et al. (2009) provided a detailed overview of the approach and demonstrate its potential through a synthetic exercise involving 30 wells and 20 surface water features. They simulated an *in situ* bioremediation operation using HPDP to study the effects of seasonal irrigation and simulate the biocurtain evolution. Although the predicted breakthrough curves matched well with observed tracer tests, the modeling application lacked calibration targets or regional data to characterize the long-term regional processes. Afshari et al. (2008) applied HPDP to a suite of synthetic examples of complex wellfields, including a 2D simulation of a confined aquifer containing several wellfield clusters. The simulated drawdowns were consistent with the analytical solution, i.e., the superposition of the Theis solution (Theis, 1935). A 3D transient example showed that submodels used in the hierarchical approach could reproduce drawdown results from a single fine-grid model, but at a fraction of the computational costs. Additional advantages highlighted were (a) HPDP eliminated the restrictive assumptions inherent in the analytical correction approach; (b) HPDP eliminated the data input and output difficulties in the traditional numerical correction approach; and (c) HPDP allowed for simulation of detailed well dynamics in a large regional model without solving a large matrix system. Liao et al. (in press) applied HPDP to a lake augmentation project including several surface water bodies and an extraction well. Mathematical models for surface and groundwater interactions and hierarchical parameter estimation were incorporated into HPDP. While these studies presented clear advantages of the HPDP, there is still the need for a complex field application of the approach that demonstrates the high level of detail with which design performance can be evaluated.

1.5. Study objectives

In this paper, we simulate a complex flow-field that is a result of many (>50) point source and sinks used in a pump-and-treat remediation operation. The specific objective of the study are to (1) verify that hierarchical patch dynamics modeling can capture small-scale dynamics at various well locations while honoring the long-term regional flow patterns predicted from a reasonable and data-intensive hydrogeologic framework, and (2) demonstrate the detailed evaluation of design performance made possible when applying HPDP to simulate a groundwater remediation system.

2. Real-world example

In this section, we introduce a large groundwater pump-and-treatment remediation operation in Michigan. At this

site, a hierarchy of models was developed to simulate the groundwater system. A description of the site and its suitability for this study is described next.

2.1. Study area

The study area (Site 23) is located in an industrial region of Michigan, is approximately 150 acres in size, and is surrounded by wetlands and surface water bodies, including Lake N1, Lake N2, River N1, and Creek N2 (Fig. 1). Decades of local industrial activity including petroleum refinery operations had contaminated almost the entire site with significant soil and groundwater contamination, characterized by high concentrations of BETXs, chlorinated organic compounds, semi-volatile organic compounds, and free phases. Monitoring suggested that some contamination had migrated off-site.

Since 2000, the State of Michigan has operated and maintained a pump-and-treat remediation system on-site, seeking to hydraulically contain the contamination, minimize off-site impact, recover free products, and ultimately cleanup the contamination. The remediation system is composed of a large network of 59 low-capacity extraction wells (6.5–65 m³/d), an extraction trench system, 10 injection trenches, two 227 m³ above-ground bioreactors, and one 227 m³ gallon clarifier tank (Fig. 1 inset). The extracted groundwater is treated on-site in the bioreactors and

clarifier tank prior to being re-injected into the ground through infiltration trenches. The network was designed to operate at a total flow rate of approximately 1637 m³/d. Although the precise extent of contamination was not known, the remediation system was designed to prevent contaminant from moving off-site.

2.1.1. Need for multi-scale modeling

The groundwater flow in the area is characterized by the complex interplay of significant variability across disparate length scales. These include variations at well-scale, site-scale, and regional scale. At the well-scale, pumping by extraction wells across the site creates a network of small drawdown cones, each with a characteristic length scale of 0.3–1.5 m. At the site-scale, the combined effects of aggregated pumping, injection, natural recharge, drainage to extraction trenches, surface seeps, local wetlands, and surface water bodies creates a large and complex groundwater mound spanning thousands of feet. Regionally, groundwater flow is controlled by Lake N1 and River N1, the global sink in the River N1 watershed. All of the different scales of variation must be properly taken into account in order to accurately simulate the groundwater flow system and to quantify and optimize the performance of the remediation system.

Systematic sampling over the years shows that concentrations of key contaminants in many monitoring wells, especially those

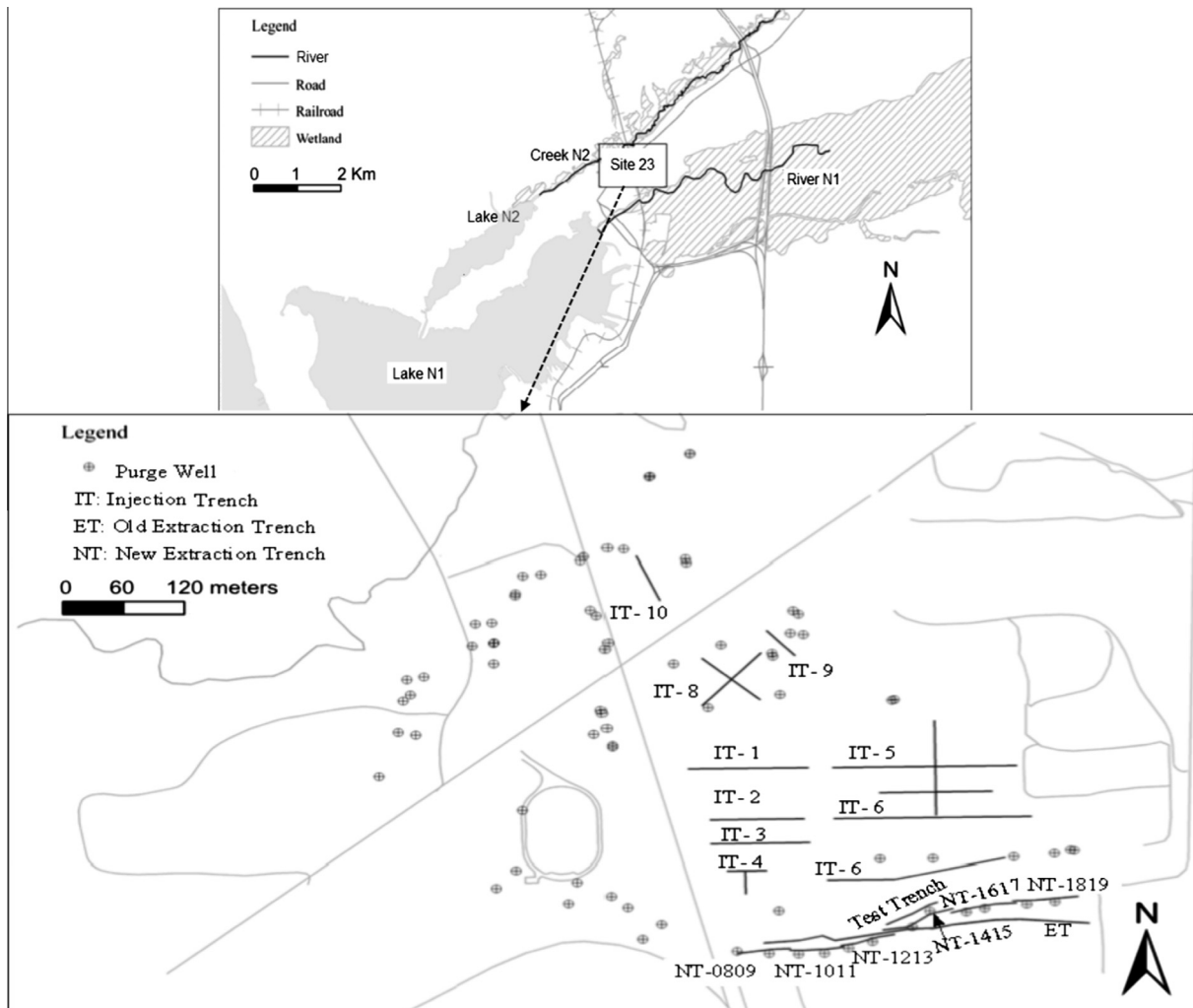


Fig. 1. Industrial region of Michigan serving as the study area, with an inset schematic of the remediation system.

in the source areas, have significantly declined. However, many questions still remain:

- How does the contamination respond to the complex pumping and injection stresses?
- Is the remediation system containing the contamination?
- Can the remediation system be optimized to significantly improve cleanup efficiency and reduce operational costs?

2.2. Conceptual representation

Our modeling effort was systematically integrated with field investigations. Data was collected on-site to specifically support the modeling study. Additional data from the Michigan state-wide geospatial databases and the state-wide groundwater database was used to construct the modeling system. The sampling network consisted of 208 monitoring wells located across the site and its immediate vicinity. Fig. 2 shows a conceptual site representation created using available data that depicts key sources and

sinks. Some of the most salient hydrological features are summarized below:

- The site is located on a topographic plateau bordered immediately by wetlands and surface waters. A cliff exists between the site in the highland area and surrounding wetlands at lower elevations (see Profile A-A' in Fig. 2). Surface seeps can be detected at the bottom of the cliff at some locations.
- The aquifer, formed of glacio-fluvial deposits such as outwash and till, has a relatively low conductivity, especially at lower elevations in the wetland area.
- The aquifer is underlain by a continuous layer of clay, providing an effective barrier to vertical migration of contaminants. The clay layer was encountered at approximately 115 boring locations and was not completely penetrated.
- The area within Site 23, being relatively flat, covered by permeable top soil and lack of vegetation, has high potential for infiltration.
- Extracted water is treated and entirely injected back into the aquifer in and around the contamination source areas.

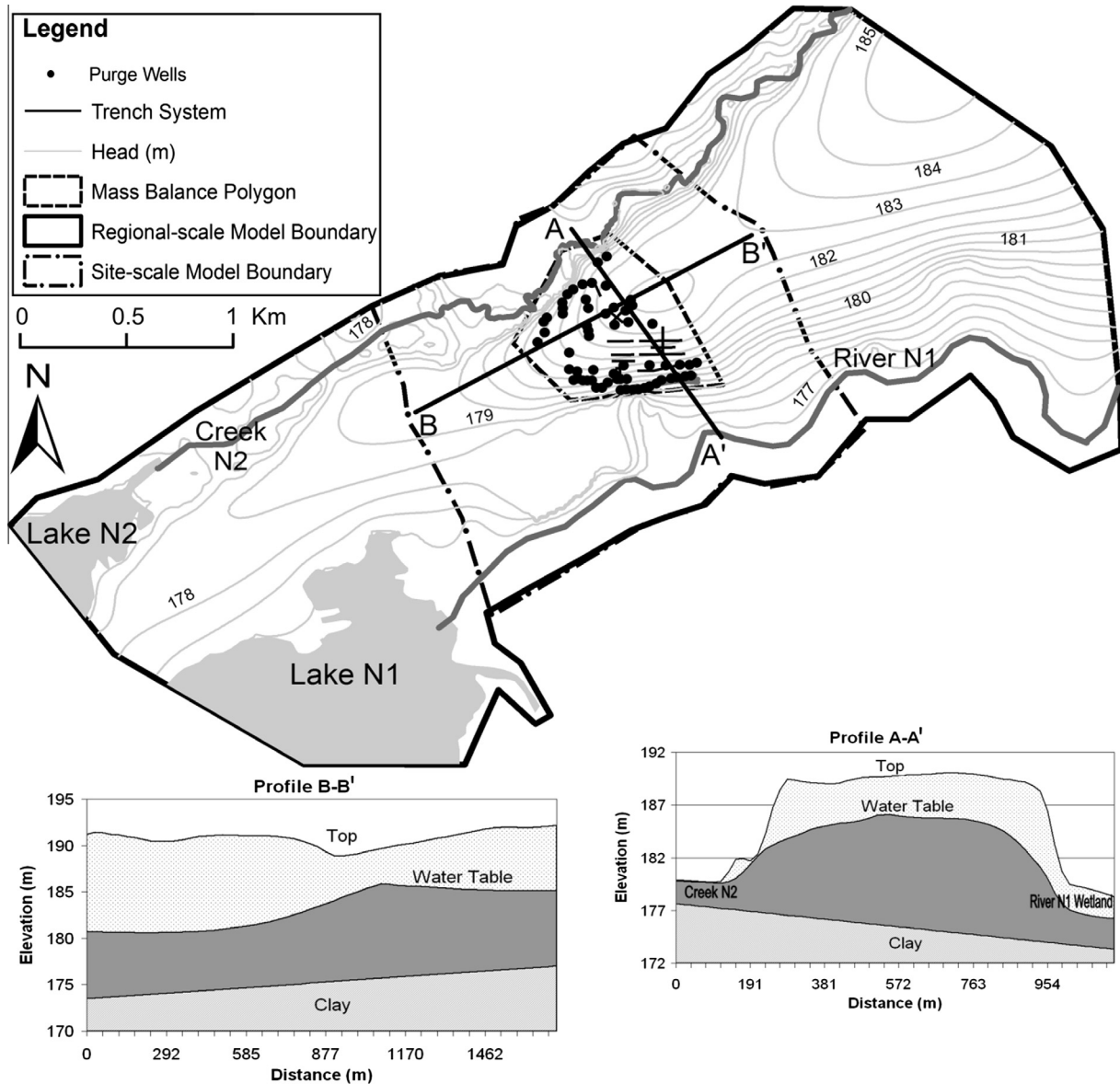


Fig. 2. Conceptual model, including regional sources and sinks.

All of this contributes to the significant, site-wide groundwater mound, with a network of “embedded” well-scale drawdown cones, resulting in a multi-scale groundwater flow system. To quantify such a complex flow system, the following sources and sinks are explicitly modeled: natural recharge, extraction wells, extraction trenches, injection trenches, Creek N2, Lake N2, River N1, Lake N2, surface seeps, and wetlands.

The highly variable terrain in the model area is represented using the 10 m high-resolution Digital Elevation Model (DEM). The land surface is treated as a drain boundary, allowing groundwater to discharge to surface where groundwater level intercepts the land surface. The drain elevation is set to be equal to the detailed, DEM-based land surface elevation. All major surface water bodies, including River N1, Lake N1, Creek N2, and Lake N2, are represented as constant head boundaries, with the water levels assumed to be approximately equal to the DEM elevations. The River N1 wetlands, Creek N2 Wetlands, and other surface seeps were represented as part of the land surface drains.

A total of 55 out of the 59 extraction wells are currently in operation and are included in the model. Although pumping rates of extraction wells vary at times, these slight changes were not represented as we focused on long-term mean conditions. The extraction trench system, including both the new and old trenches, is modeled as line drains, or head dependent fluxes. The new trenches are relatively deep (4.3 m) but narrow (0.3 m) while the old trench is shallow (1.2 m) but wide (0.9 m). The injection trenches – 8 in the southern part of the site and 2 in the north – are represented as line sources with prescribed fluxes. The injection trenches are filled with highly permeable peat and gravel and treated water is continuously injected to the trench through a well. The prescribed flux per unit length is set to be equal to the injection rate of the injection well divided by the length of the trench. The flux values for all injection and extraction trenches under current design conditions are presented in Tables 1 and 2, respectively. The total injection rate into all the injection trenches is equal to the total pumping rate from all the extraction wells and trenches.

Natural recharge is modeled as a spatially variable quantity and is divided into five zones based on land-use. The five recharge zones are: the site, two residential districts on the plateau (NE and SW side of the site), the River N1 wetland area, and the Creek N2 wetland area. Hydraulic conductivity is divided into three zones based on the geologic information of the aquifer material and the Michigan land-system information available from the statewide groundwater database. The different recharge and conductivity zones are shown in Fig. 3.

The clay layer underneath the aquifer is assumed to be impervious. The clay elevation was interpolated using universal Kriging with a linear drift. The north-eastern model boundary is selected such that it coincides with a streamline and can thus be approximately represented as a no-flow hydraulic boundary. The “remote”

Table 2
Pumping rates for extraction trenches.

Extraction trench	Pumping rate (cubic meters per day)
NT0809	0
NT1011	–17
NT1213	–39.9
NT1415	–17.7
NT1617	–49.8
NT1819	–42.6
Old extraction trench	–419
Test trench for free product	–15.7

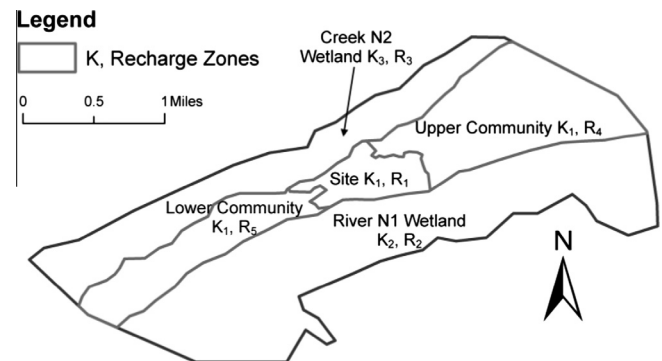


Fig. 3. Recharge and conductivity zones within the modeling domain.

streamline is delineated based on regional static water levels from the Michigan statewide groundwater database.

3. Hierarchical flow modeling

Under the HPDP, we modeled the complex flow system incrementally, visualize the results in real-time, and zoom into sub-areas when and where we feel there is a need to. We made use of Interactive Groundwater (IGW), developed by Li and his co-workers as the modeling environment for HPDP (Li and Liu, 2006a,b, 2008; Li et al., 2006). Groundwater flow is modeled as unconfined and two-dimensional. Slight vertical variation in the center of the mound and in the discharge area is ignored. The algorithms for up- and down-scaling between models at different spatial scales, as well as the discretization, numerical scheme and grid layout in the various model levels have not previously been published and are therefore provided in Appendix A.

We begin with modeling the entire study area using a coarse grid and then make localized corrections by adding patches or patches-in-a-patch (sub-models nested within sub-models). The boundary conditions for each new sub-model were represented as prescribed heads and $H_c = H_p$ for shared nodes, where H_c and H_p is the head in the child model and parent model, respectively. Up to three levels of sub-models were created with spatial step size of 7.6 m, 1.5 m, and 0.5 m, respectively. At each level, multiple patch models were created. The level I model represents the regional model described above. The level II model is the first level of sub-model that uses the prescribed heads simulated in the level I model. Similarly, level III models were created using prescribed heads at the boundaries simulated in the previous level of the model. For this study, no feedback loop is considered between parent models and their nested sub-models (i.e., only one-way, down-scaling interaction is implemented). A visual sensitivity analysis is used to evaluate the sufficiency of the patch boundary location. Model results, including calibration, sensitivity analysis, and applications to remediation performance evaluation are presented in the sections that follow.

Table 1
Pumping rates for injection trenches.

Injection Trench	Pumping rate (cubic meter per day)
IT-1	34.6
IT-2	134.3
IT-3	211.1
IT-4	176.6
IT-5	191.9
IT-6	214.9
IT-7	207.3
IT-8	157.4
IT-9	168.9
IT-10	130.5

Table 3
Calibrated values of hydraulic conductivity and recharge.

Location	Conductivity (m/day)	Recharge (mm/year)
Site	5.00	673.1
N1 wetland	3.28	0
N2 wetland	0.87	13.208
Upper community	5.00	323.088
Lower community	5.00	465.074

Table 4
Calibrated values of bottom elevation and leakance of trench system.

	Bottom elevation (m)	Leakance (m/day)
NT1011	178.98	8.96
NT1213	176.27	0.74
NT1415	178.07	0.35
NT1617	178.08	0.81
NT1819	178.08	0.61
Test trench	178.91	0.32
Old trench	176.98	6.83

3.1. Model calibration

The groundwater flow model was calibrated under steady-state conditions. One site-scale model was created with boundaries perpendicular to the head contours generated by the regional-scale model (see Fig. 2). The calibration was performed based only on the site-scale model. The calibration parameters were the conductivity and recharge values in the different zones (as seen in Fig. 3), the bottom elevation and the leakance coefficient of the new extraction trenches, the old extraction trench and the test trench of free product. The calibration targets were the static water levels collected at 208 monitoring wells throughout the site on May 12, 2010 with the remediation system turned on and seepage flux from 4 new trenches, the test trench and the old extraction trench. Applying UCODE (Hill and Tiedeman, 2007), calibration was achieved by minimizing the Sum of Squared Differences between the simulated and observed heads, and simulated and observed fluxes. The automatic parameter estimation took approximately 20 h on a single 3 GHz processor on a Dell® CPU operating on the Windows 7 system.

The final calibrated conductivities and recharge are presented in Tables 3 and 4. The distribution of calibrated values for recharge,

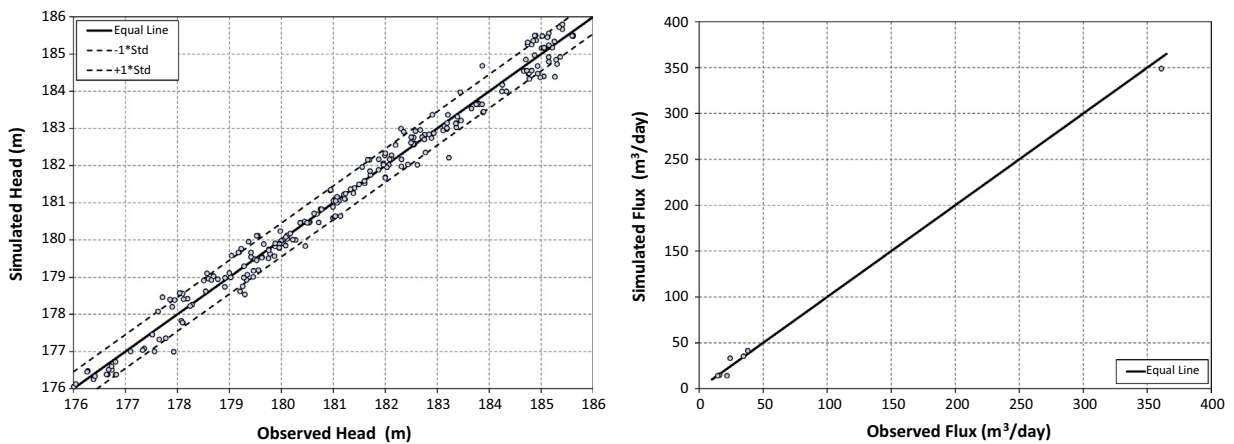


Fig. 4. (left) A comparison of simulated and observed heads at steady-state for 208 monitoring wells. (Right) A comparison of simulated and observed fluxes at steady-state for 6 extraction trenches.

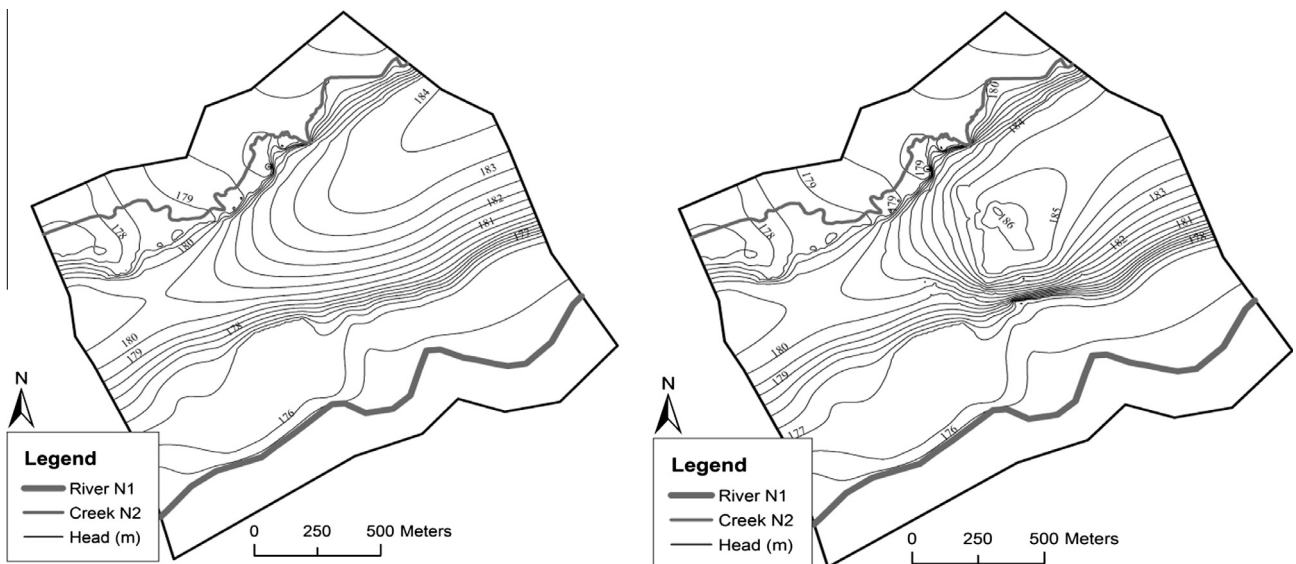


Fig. 5. (left) Steady-state head contours for an active remediation system. (right) Steady-state head contours for an inactive remediation system.

Table 5
Results of sensitivity analysis.

Parameters	Gradient
Recharge of the site	0.0407
Conductivity of plateau	0.0360
Recharge of N1 wetland	0.0170
Conductivity of N2 wetland	0.0128
Conductivity of N1 wetland	0.0103
Grid size	0.0018
Recharge of lower community	0.0006
Recharge of N2 wetland	0.0000
Recharge of upper community	0.0000

conductivity, and bottom elevation and leakance for extraction trenches was consistent with our conceptual understanding. In addition, very different initial guesses for the calibration parameters lead to essentially the same estimated values for recharge and conductivity. The bullets below provide additional comments on the calibrated recharge values:

- Estimated recharge at the site polygon was significantly higher than the estimated values in the residential areas and in the wetland areas, which is consistent with our conceptual model.
- The site polygon recharge of 673.1 mm/yr is about 78% of the annual average precipitation of 877 mm/yr (National Weather Service). This is reasonable given the potential for high infiltration at the site as noted earlier.

- A negligible net recharge to the wetland is plausible because it reflects the fact that water coming into the wetland is consumed by the vegetation in the form of ET (not explicitly modeled).

Fig. 4 presents the comparison of observed and simulated heads and fluxes at steady-state for 208 monitoring wells and 6 extraction trenches in the site-scale model, respectively. The predicted head and flux distributions match well with the observed values. The RMS error of head is approximately 0.30 m or 3% of the maximum observed head difference across the site. The arithmetic mean error is almost zero at 0.01 m or 0.1% of the maximum observed head difference. The errors at the vast majority of the 208 monitoring wells are within one standard deviation.

The time scale in groundwater remediation is O (decades). Therefore, the goal of the modeling effort was to simulate long-term average processes relevant to the pump-and-treat system. Ideally, long-term data would be used to calibrate a steady state model, but is oftentimes not practical because data that reflects the long-term mean of a spatial pattern is seldom available. The dataset from May 12, 2010 was the only dataset available during the modeling effort. Also, sampling during the month of May is representative of the time of the year when the groundwater mound is at or near its highest and resulting pore velocities are at or near their fastest. Under such conditions the predicted capture zones are narrower; thus, this approach provides a conservative estimate of the remediation system’s ability to capture all of

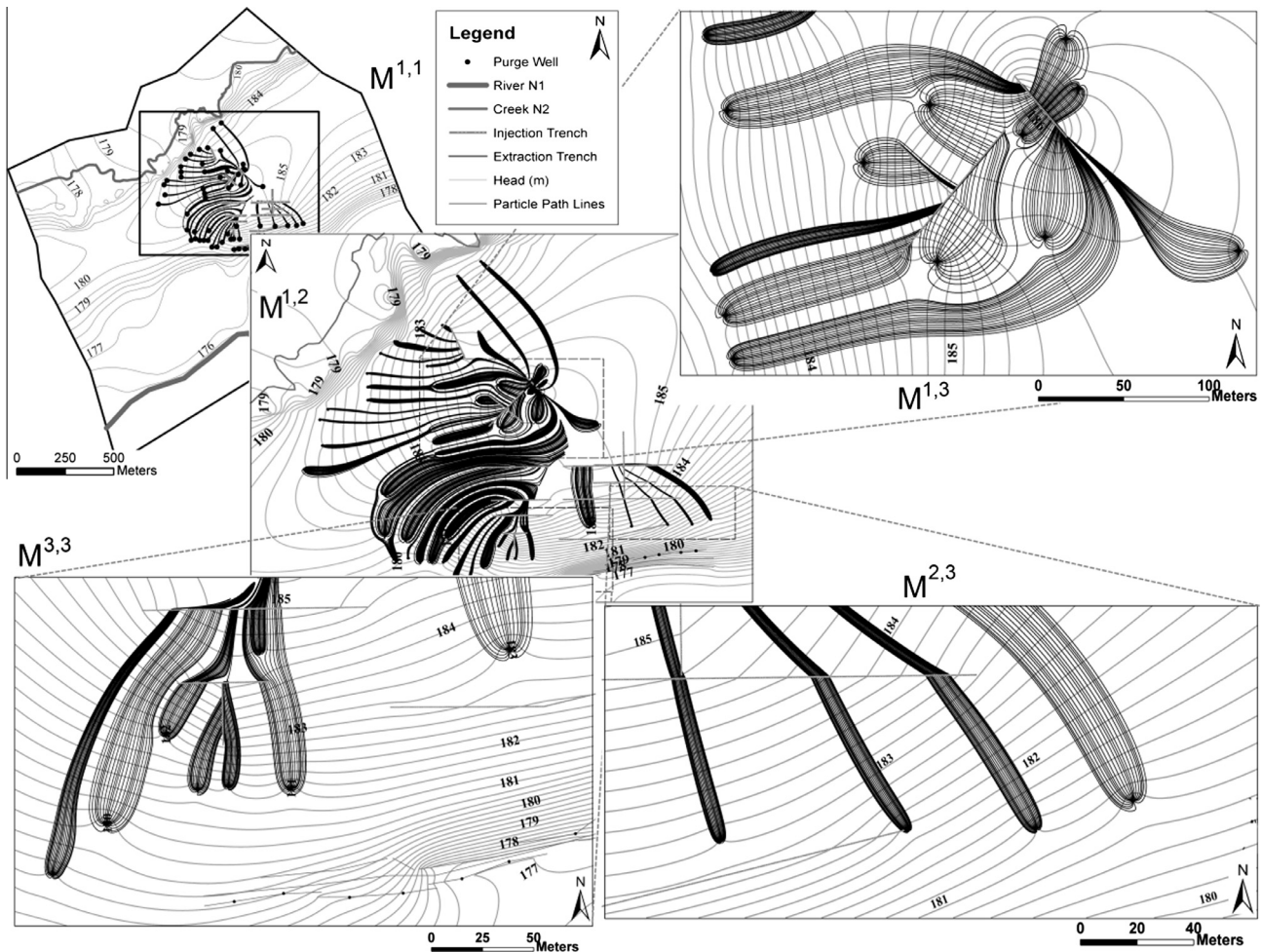


Fig. 6. Hierarchical reverse particle tracking from patch model $M^{1,2}$ and its patch models $M^{1,3}$, $M^{2,3}$ and $M^{3,3}$.

the on-site contamination. Fig. 5 provides the calibrated head and flux distribution at steady-state with the system on and the system off, respectively, demonstrating the changes in head distribution at the site.

3.2. Model sensitivity analysis

A sensitivity analysis of the steady-state model was conducted to assess the uncertainty in the input values. The analysis was used to determine if the difference between the simulated and observed data values could be accounted for by the range of uncertainty in the values of input parameters. This analysis provided a measure of the sensitivity of the model results to changes in the values of key parameters and, thus, provided a check on the calibrated model. Throughout the model area, the principal input parameters were independently decreased by a constant factor of 2%, while other parameters were left unchanged. The gradient of the objective function based on these parameters was used as a measure of sensitivity. A summary of the gradient for all parameters is included in Table 5. The analysis indicated that model simulations are most sensitive, in decreasing order of importance, to (a) the conductivity of the site and the lower community, (b) the conductivity in the River N1 wetland area and (c) recharge of the site and the upper community, respectively. Other parameters – including grid size, conductivity of Creek N2 wetland, and recharge in the lower community and Creek N2 wetland – had a relatively small influence.

4. Model applications

In this section, we take advantage of the model's ability to simulate not only large-scale dynamics, but also detailed near-well dynamics, to investigate systematically the remediation system performance at Site 23. We begin with an analysis to quantify the capture zones for the extraction system. We achieve this by performing reverse particle tracking for all capture wells based on hierarchically-modeled velocity fields. Although accounting for small-scale spatial variability is important for particle tracking, the use of stochastic modeling is beyond the scope of this study. Capture zones tend to get dispersed (larger) as a result of small-scale heterogeneity (Anderson and Woessner, 1992). Since we did not represent small-scale heterogeneity in our models our particle tracking analysis is conservative, which is appropriate for management of contaminated groundwater that must be kept from spreading.

4.1. Hierarchical capture zone analysis

Figs. 6 and 7 present results from hierarchical reverse particle tracking. Although the models were developed hierarchically at multiple resolutions, only the ones at the finest resolution properly represent the rapidly-varying well dynamics and their capture zones. The level I model, at a resolution of 7.6 m, was only sufficient for delineating the general orientation of the capture zones. The level 2 model, at an improved resolution of 1.5 m, can be used

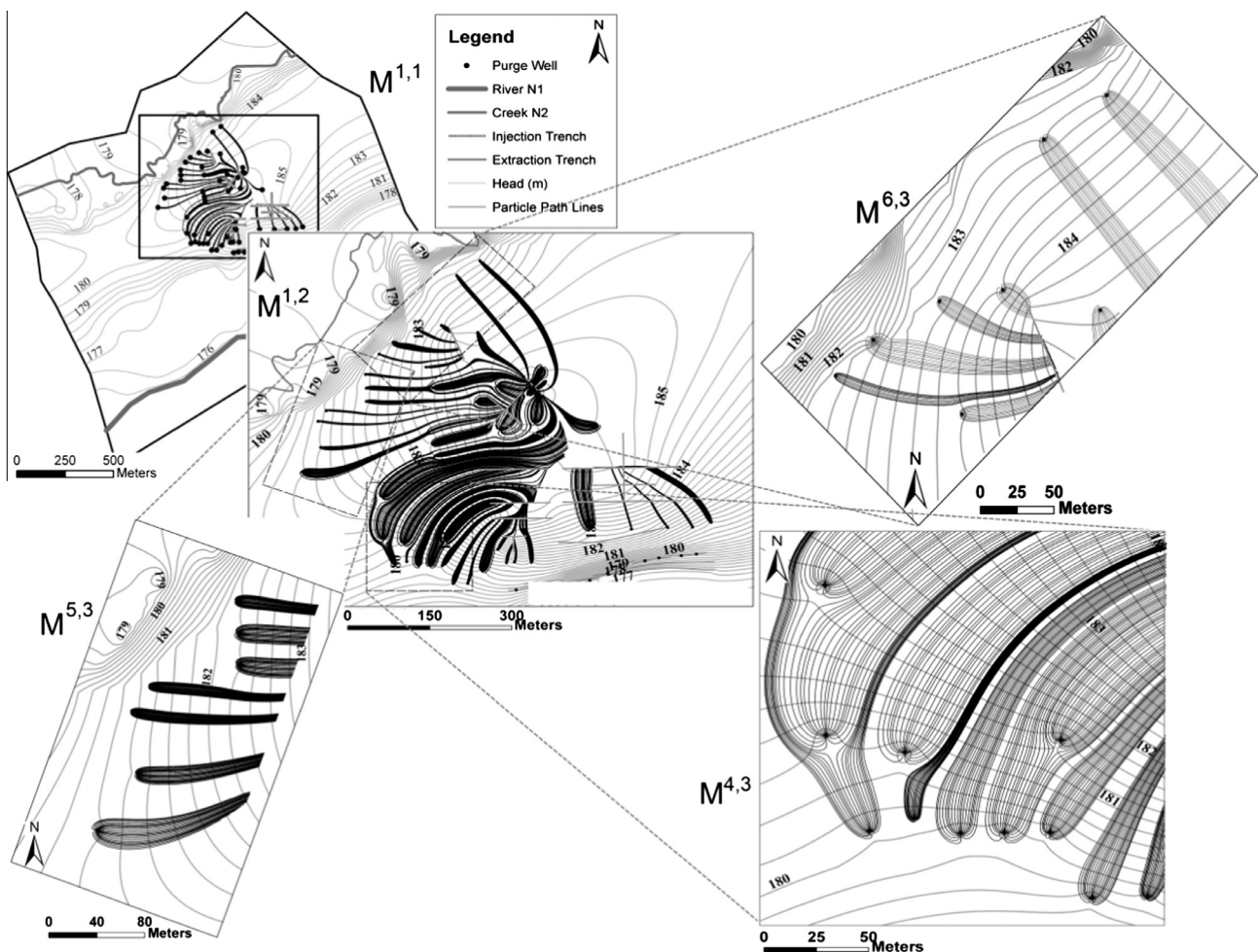


Fig. 7. Hierarchical reverse particle tracking from patch model $M^{1.2}$ and its patch models $M^{4.3}$, $M^{5.3}$ and $M^{6.3}$.

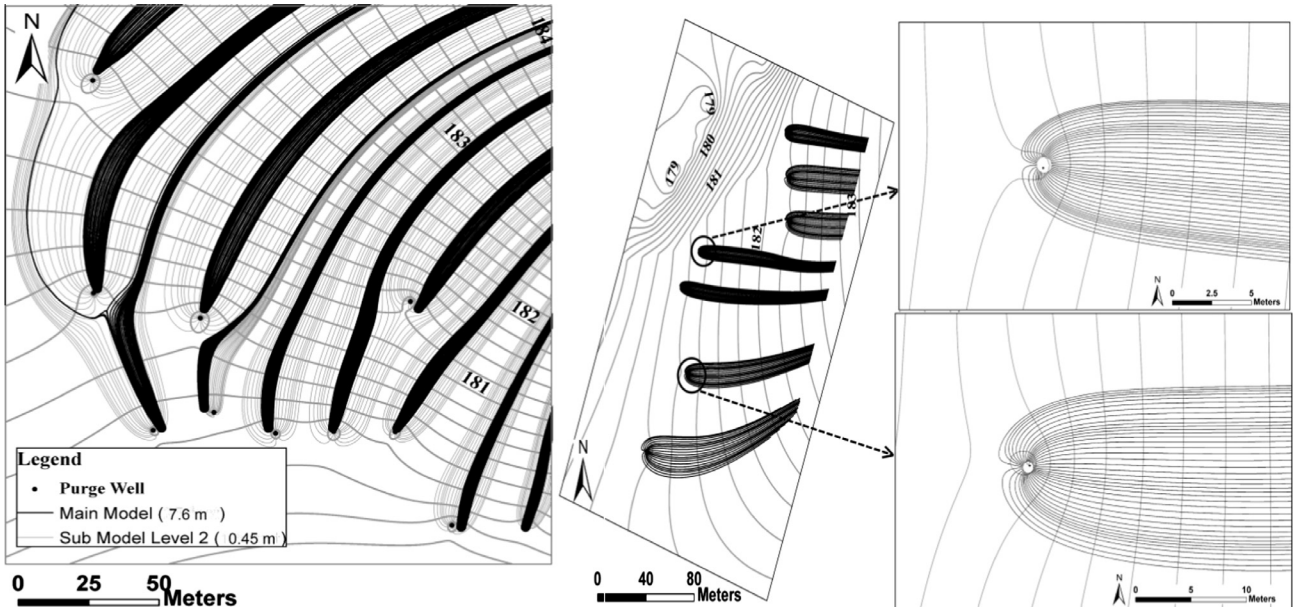


Fig. 8. (left) Detailed capture zones at relatively high ($\sim 65\text{ m}^3/\text{d}$) pumping rates. (right) Detailed capture zones for wells with pumping rates less than $33\text{ m}^3/\text{d}$.

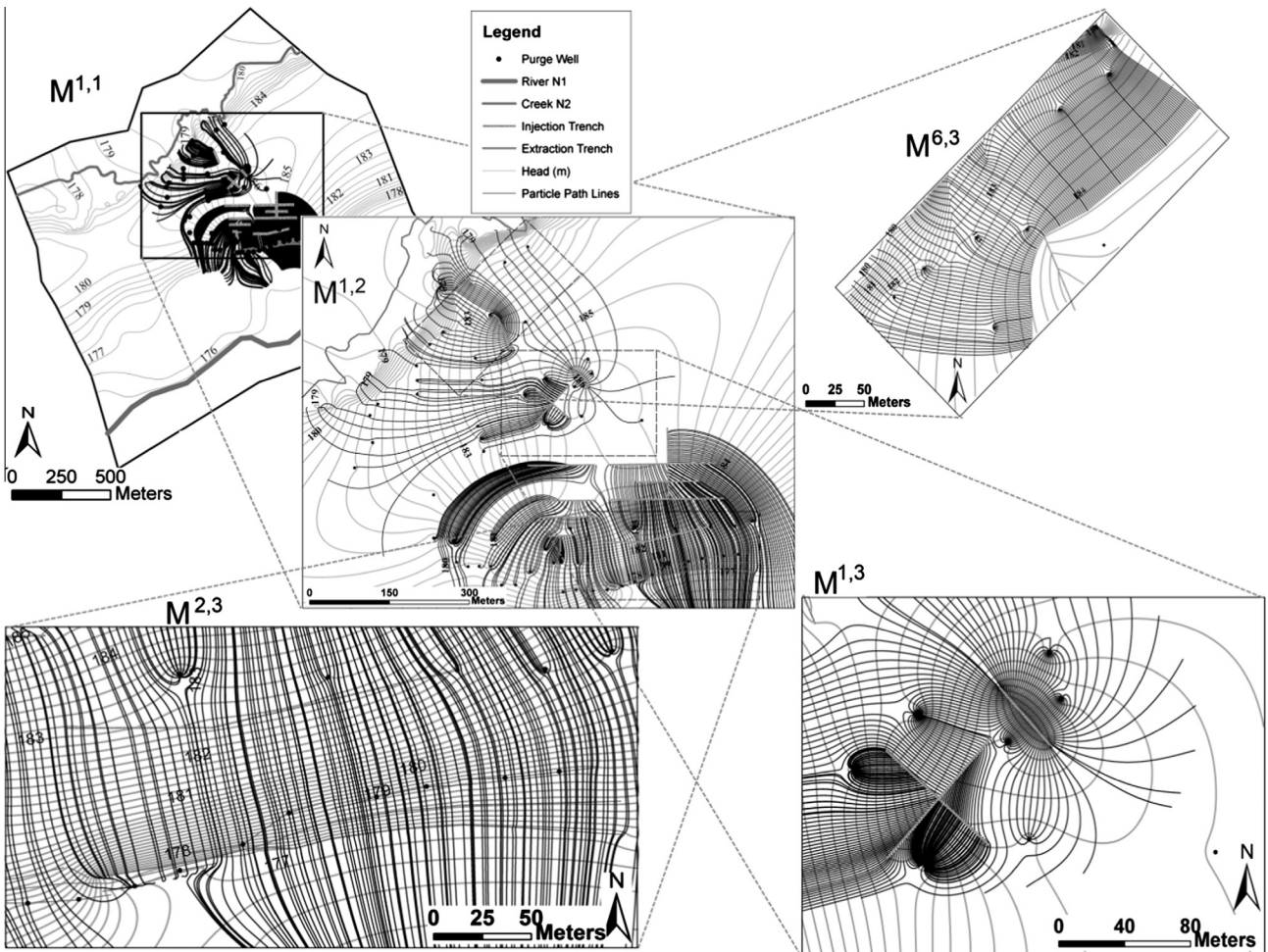


Fig. 9. Hierarchical forward particle tracking for model $M^{1,1}$, sub-model $M^{1,2}$, and sub-sub-models $M^{6,3}$, $M^{1,3}$ and $M^{2,3}$.

to delineate the general outline of the capture zones, but significantly underestimated the capture widths. Zooming into six focused areas at a substantially refined resolution of 0.5 m, level III models resolved detailed capture zones for wells that pump at relatively high rates – close to 65 m³/d and made it possible to delineate small-scale drawdown cones of depression and the associated capture zones, even for wells with pumping rates less than 33 m³/d in a large and complex model (Fig. 8).

The hierarchical modeling results clearly show the challenges in containing the contamination at Site 23, given the small sustainable extraction rates and diverging flow patterns. The models show that significant gaps exist in the current capture system despite the large number of extraction wells utilized. The area that is most problematic is the northern side of the site where the well distribution is relatively sparse and hydraulic gradient is strong. The widths of the predicted gaps between individual capture zones range from 31 to 152 m.

The models predict even wider gaps in the well capture zones on the south side of the site (i.e., north of the cliff) where the hydraulic gradient present is strongest. However, this area, unlike the northern side, is also protected by a series of “new” and “old” extraction trenches further downstream. Contamination that escapes the wells can potentially be captured by the extraction trenches. The effectiveness of the trench system is further

evaluated in the next section. Based on the model prediction, the area that is best protected is in the southwest portion of the site where the well distribution is dense and the pumping rates are high. Individual capture zones for the different wells overlap to form a large and contiguous capture zone.

4.2. Hierarchical forward particle tracking

In this section, we illustrate how contamination at Site 23 can potentially migrate off-site, given the predicted gaps in the capture system. To obtain a conservative estimate of the contaminant migration, we model only advective transport, ignoring degradation and sorption. We thus exclude a discussion of the solute chemistry as it does not have any impact on the overall modeling objective. Particles were released throughout the site where data show elevated contaminant concentrations, and used forward particle tracking to simulate contaminant migration under steady flow conditions.

Using parallel processing with sixteen 3 GHz processors on the same Dell® units, the particle tracking took approximately 3–4 h. Figs. 9–11 present the final hierarchical forward particle tracking solutions presented in 8 patch models across 3 levels. M¹ shows the regional solution at the top of the hierarchical-tree. M^{1,2} describes the sub-regional dynamics and well-field interactions

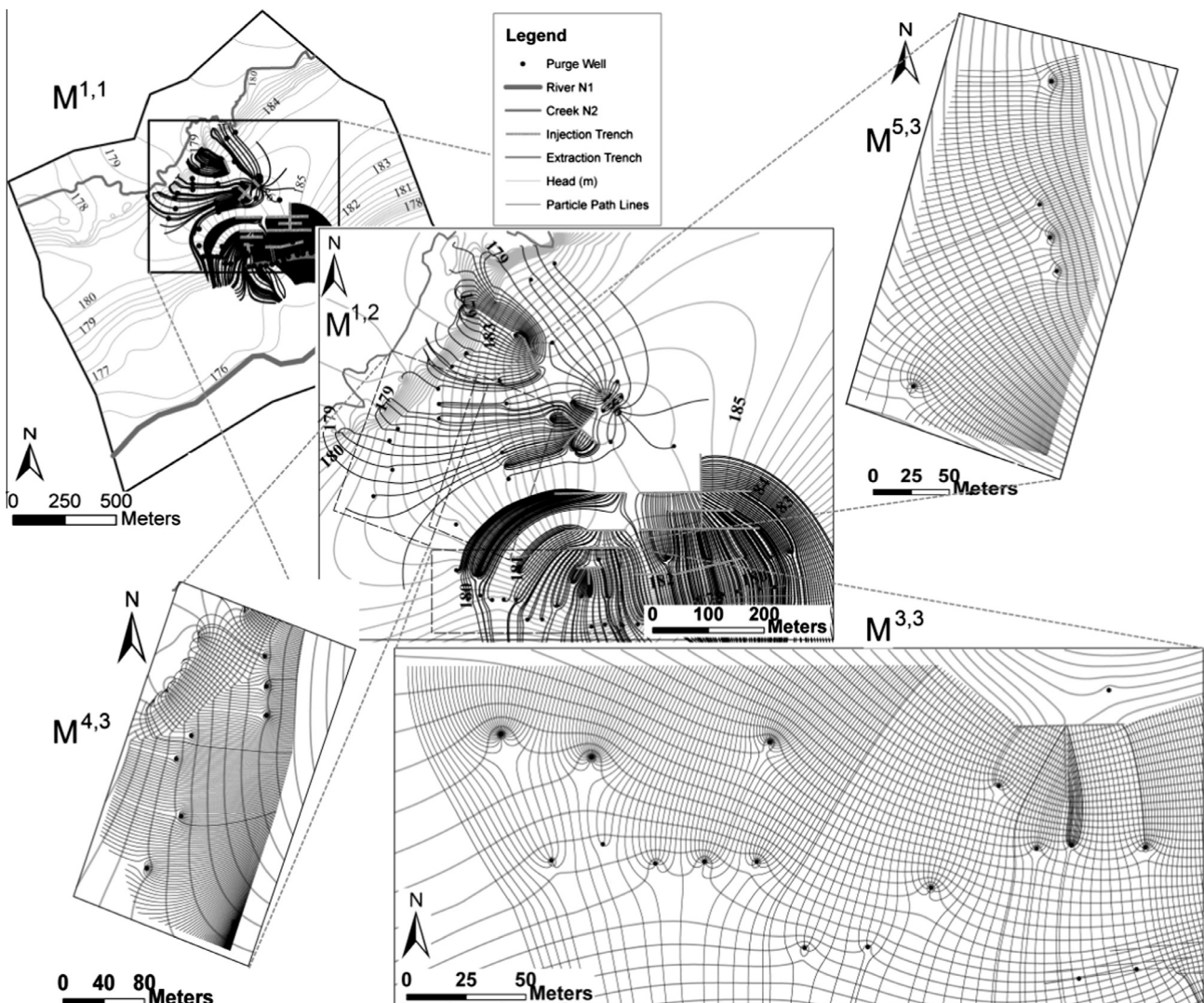


Fig. 10. Hierarchical forward particle tracking for model M^{1,1}, sub-model M^{1,2}, and sub-sub-models M^{3,3}, M^{4,3} and M^{5,3}.

in more detail. $M^{1,3}$ to $M^{6,3}$ in Figs. 9 and 10 present a sub-sub-model for each well-field, capturing more detailed well interferences. The remaining subplots (Fig. 11) present a series of patch-models zooming into 2 focused-areas that play critical roles in the overall scheme of integrated management.

The models clearly show that the particles travel in all directions. The most dominant migration pathways are toward the west, south, and north. The westward movement eventually branches into two directions - northwest and southwest. The northwest branch moves toward Creek N2 but stops expanding on reaching the wetland area near Creek N2. Similarly, the southwest branch moves toward River N1 but stops spreading on reaching the River N1 wetlands. Particle transport toward the south boundary is probably most intense because eight of the ten injection trenches are located on the south site and are close to the site boundary. Model $M^{3,3}$ clearly shows that particles migrate past the capture wells through the gaps between the well capture zones. The models also show that the particles that escape the capture wells proceed past the new trenches and old capture trench before being captured by the River N1 wetlands.

Particle transport toward the north boundary is also significant because Creek N2 bends toward the site and is closest to contamination at the junction where Little Creek N2 and Creek N2 meet. At this location Creek N2 almost directly borders the site with virtually no buffer zone in between. Model $M^{5,3}$ shows that particles eventually expand into Little Creek N2, which is connected with Creek N2, and finally move toward Lake N2 at the downstream reach.

The models also show that particles released at the site migrate east in a direction opposite to the natural regional gradient. The east movement also bifurcates in two directions: northeast toward Creek N2 and southeast toward River N1. However, movement in both directions stops in the wetland areas near Creek N2 and

River N1. It becomes clear that the wetlands on both sides of the site act as buffer zones that absorb contamination and arrest its further migration.

4.3. Water balance analysis

In this section, we quantify the total seepage flux moving off-site. We achieve this by creating a water budget for the aquifer within the site area. The budget analysis is performed based on modeling results, both under natural and active remediation conditions. The mass balance polygon is shown in Fig. 2, and the results of the analysis are presented in Fig. 12.

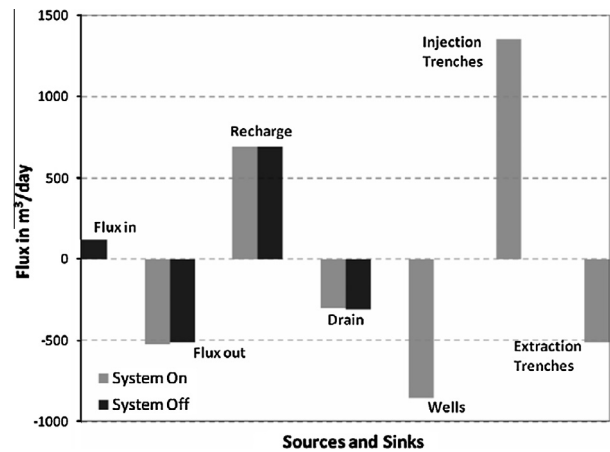


Fig. 12. Water budget analysis for the site area.

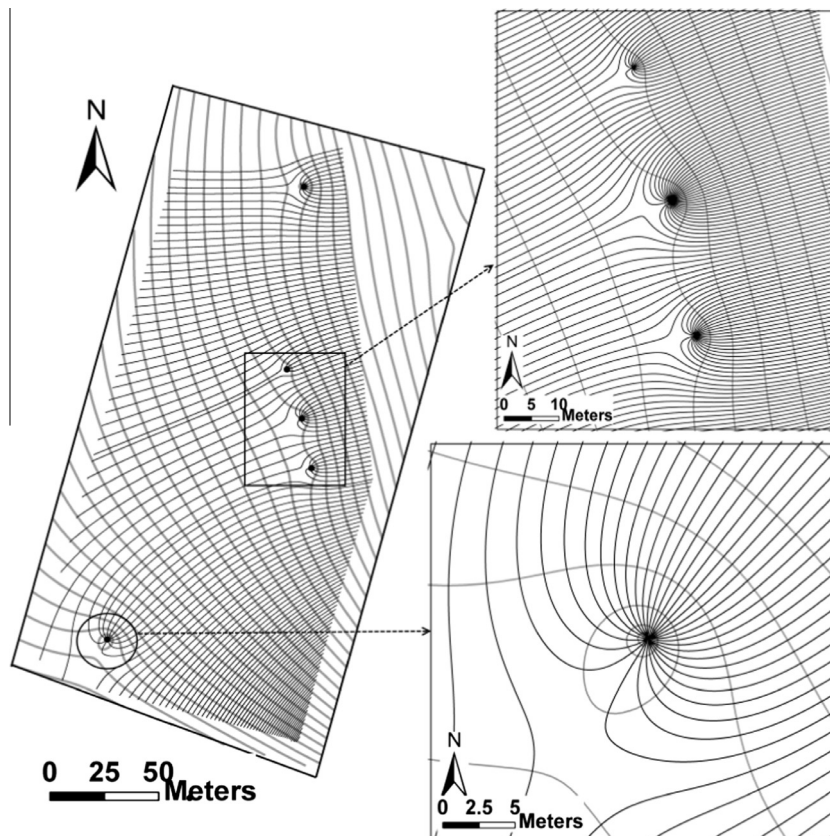


Fig. 11. series of patch-models zooming into 2 focused-areas that play critical roles in the overall scheme of integrated management.

One significant message from the budget analysis is that the seepage flux off-site remains almost the same with or without remediation, and is approximately equal to natural recharge in the site area. Specifically, the predicted seepage flux out of the site boundary was approximately 349 m³/day without the remediation system turned on and approximately 356 m³/day otherwise.

This finding, although initially puzzling, becomes immediately obvious upon a closer examination of the water budget. The flux off-site does not significantly change simply because what is pumped out by the wells is injected back into the ground through the injection trenches within the same area. Under natural conditions, steady-state flow out of the site is essentially balanced by natural recharge, since other sources and sinks (e.g., inflow from the boundaries and surface seeps) are relatively small. Under active remediation, the flow off-site is still balanced by natural recharge, since total injection on-site is designed to be equal to total pumping, and boundary inflows and surface seeps are again relatively small. Of course, the quality of the water moving off-site with and without remediation should be significantly different, and contaminant flux off-site should decrease with time.

5. Conclusions

In this paper, we demonstrate the potential of HPDP by investigating the impact of the current remediation system on the groundwater flow and contaminant migration at Site 23 in Michigan. A hierarchical groundwater modeling system was created to critically evaluate the efficiency and effectiveness of the remediation system. The flow system was especially complex owing to a multitude of extraction wells and injection trenches, a number of different hydraulic features, and various land covers encountered regionally. The model was calibrated with water level measurements from 208 monitoring wells and seepage flux from 6 trenches. Hierarchical reverse particle tracking revealed that significant gaps exist between purge-well capture zones, contributing to leakage of the contaminant. Hierarchical forward particle tracking showed that contamination that escapes capture was eventually “arrested” by the River N1 and Creek N2 wetland system. Water balance analysis based on the modeling results showed that seepage flux off-site is almost equal for active and inactive remediation conditions.

These insights illustrate the detail in which design performance can be evaluated when applying HPDP to simulate a real-world groundwater remediation system. Furthermore, this modeling application reinforces the following advantages of utilizing HPDP for multi-scale modeling of real sites with complex field environments:

- A high degree of detail can be captured in any area of interest in the study area, and local solutions are physically consistent with the regional solutions.
- Complex particle tracking can be applied to any scale or location and remain consistent with larger- or smaller-scale dynamics.
- Data from multiple scales of interest can be integrated to make full use of the information available for groundwater modeling.

Most importantly, each of the above-mentioned advantages are made possible without exceeding the computational limits of a modest processing system or requiring extensive data management efforts. Thus, the HPDP approach provides an opportunity to analyze complex hydrological field environments in a pragmatic, time-efficient manner.

Acknowledgement

The authors kindly thank the Michigan Department of Environmental Quality (MDEQ) for funding this research.

Appendix A. Core of the HPDP approach

A.1. Governing equations and algorithms

For a generic model, $M^{p,l}$, which refers to model patch p in level l , the governing equations can be given as:

$$S_s^l \frac{\partial H^l}{\partial t} = \nabla \cdot (\underline{K}^l \cdot \nabla H^l) + q^l \tag{A.1}$$

With down-scaling BC: $H^l|_{\Gamma_1^l} = f(H^{l-1}|_{\Gamma_1^l})$ or $(\underline{K}^l \cdot \nabla H^l) \cdot \vec{n}|_{\Gamma_1^l} = (\underline{K}^{l-1} \cdot \nabla H^{l-1}) \cdot \vec{n}|_{\Gamma_1^l}$

up-scaling BC: $H^l|_{\Omega_1^l} = f(H^{l+1}|_{\Omega_1^l})$ or $(\underline{K}^l \cdot \nabla H^l) \cdot \vec{n}|_{\Gamma_2^l} = (\underline{K}^{l+1} \cdot \nabla H^{l+1}) \cdot \vec{n}|_{\Gamma_2^l}$

IC: $H^l(\vec{x}, 0) = H^{l-1}(\vec{x}, 0)$

where S_s is the specific storage coefficient, H is the hydraulic head, t is time, ∇ is the gradient operator, \underline{K} is the saturated hydraulic conductivity tensor, q represents source (positive) or sink (negative) terms including pumping/injecting wells, streams, lakes, drains, etc.; Γ_1 is the computational domain boundary between $M^{p,l}$ and its parent model, Γ_2 is the computational domain boundary between $M^{p,l}$ and its child model, Ω_1 is the computational domain of the child model, f is a generic function, \vec{n} is the normal vector to the parent-child boundary, and \vec{x} is the spatial vector. The superscript l refers to the model level for the current patch, with parent model at level $l - 1$ and child model(s) at level $l + 1$. The naming convention used here is described as:

- **Main model:** The top-most level ($l = 0$) model, referred to as the regional model.
- **Parent model:** A model at any level ($l = 0, 1, \dots, L - 1$) that has at least one child model.
- **Child model:** A model at any level ($l = 1, 2 \dots L$), which has a finer grid than its parent model. Also referred to as a patch model, and can have only one parent model. Orphan models (i.e., child models without a parent model) are not allowed as boundary conditions cannot be imposed on such models.

In general, boundary conditions (BCs) and initial conditions (ICs) are only provided for the main model (i.e. the largest scale model). In order to obtain solutions for models at other levels, their BCs and ICs are imposed from their respective parent models as explained below:

- (1) With the given BCs and ICs, main model can be solved numerically and its head, H^0 , will be obtained throughout the whole computational domain.
- (2) Head, $H^1|_{\Gamma_1}$, along the interfaces of main model and its child models (patches) can be interpolated from H^0 ; also, fluxes, $(\underline{K}^1 \cdot \nabla H^1) \cdot \vec{n}|_{\Gamma_1}$, crossing these interfaces can be calculated from H^0 . ICs for child models can be obtained by interpolating heads inside their domains from H^0 .
- (3) The procedure of solving for the heads of a model at level l by obtaining BCs and ICs from its parent model at level $(l - 1)$ is repeated until $l = L$. This procedure is called down-scaling. After the heads, H^L , in the last model level have been calculated, they are used as the base heads to

update the heads along the child–parent interfaces. This will result in a change in the BCs of the parent models (upper level models): $H^{l-1}|_{r_2}$ or $(\underline{K}^{l-1} \cdot \nabla H^{l-1}) \cdot \vec{n}|_{r_2}$ along the interfaces of parent–child models will be calculated from their child model’s head, H^l , and thus, H^{l-1} will be updated. This procedure is repeated until main model ($l = 0$) is reached. This procedure is called up-scaling.

- (4) Steps (1) to (4) are repeated until the maximum head difference between consecutive iterations meets a given convergence criterion. When the system converges, the whole modeling system is stopped.

A flow chart of the down- and up-scaling procedures in the hierarchical modeling system is shown in Fig. A.1.

A.2. Discretization and numerical scheme

Solving Eq. (A.1) numerically involves discretizing the Partial Differential Equation (PDE) in a computational domain to form a linear algebraic system with head at each discretized node as the unknown. In our hierarchical modeling system, the computational domain is discretized with no gaps nor overlapping bricks (3D) or rectangular (2D) cells, and with nodes at the center of cells (Fig. A.2). Fig. A.2 shows a typical cell of node P and its neighboring nodes E, S, W, N, T, B . Lines connecting node P and its neighboring nodes E, S, W, N, T, B have intersection with cell-faces at face node e, s, w, n, t, b , respectively. The PDE is approximated in each cell by using finite volume method (FVM) to yield a node-based discretized equation:

$$A_P H_P^{m+1} + A_E H_E^{m+1} + A_W H_W^{m+1} + A_N H_N^{m+1} + A_S H_S^{m+1} + A_T H_T^{m+1} + A_B H_B^{m+1} = S_r \tag{A.2}$$

where

$$\begin{cases} A_E = -\frac{\Delta S_e K_e}{\delta_{EP}}, & A_W = -\frac{\Delta S_w K_w}{\delta_{PW}}, & A_N = -\frac{\Delta S_n K_n}{\delta_{NP}}, & A_S = -\frac{\Delta S_s K_s}{\delta_{PS}} \\ A_T = -\frac{\Delta S_t K_t}{\delta_{TP}}, & A_B = -\frac{\Delta S_b K_b}{\delta_{PB}}, & S_r = S_C \Delta V_i + \frac{S_s \Delta V_i}{\Delta t} H_P^m \\ A_P = -(A_E + A_W + A_N + A_S + A_T + A_B) + S_p \Delta V_i + \frac{S_s \Delta V_i}{\Delta t} \end{cases} \tag{A.3}$$

and $\Delta S_e, \Delta S_w, \Delta S_n, \Delta S_s, \Delta S_t$ and ΔS_b are the areas of the cell-faces: e, w, n, s, t, b ($\Delta V_i = \Delta S_e \Delta S_n \Delta S_t = \Delta S_w \Delta S_s \Delta S_b$). Accordingly, K_e, K_w, K_n, K_s, K_t and K_b are conductivities evaluated on the cell-faces of e, w, n, s, t, b respectively. The distance from node i to node j is given by δ_{ij} , m denotes the time level, and Δt is the time step. If q is a head-dependent source/sink, then it can be linearized as: $q_P = -S_p H_P^{m+1} + S_C$, where S_p and S_C are the slope and the intercept of the linearization, respectively.

A.3. Grid layout design

In this hierarchical modeling approach, information propagates in both down- and up-scaling directions through the parent–child model interfaces. Information propagation from parent to child model involves passing information from a coarser to a finer grid and vice versa. Therefore, a well-designed grid layout (including temporal gridding) can propagate information accurately and efficiently. Interpolation schemes, both spatial and temporal, also depend on the grid layout.

The grid layout is based on shared-nodes, which are those nodes that are shared by both parent and child models such as node A, B, C and D in Fig. A.2. Nodes A' and B' are not shared nodes. Connecting the shared nodes on the child model boundary will form the interfaces of the parent and child models such as line AB in Fig. A.2. In other words, a child model’s boundaries are a part of the parent model’s grid lines. This grid configuration greatly simplifies the interpolation efforts – which are used very intensively in down- and up-scaling iterative loops in hierarchical modeling – and therefore, can save computational time considerably.

A.4. Boundary condition propagation between parent and child models

Child models contain finer grid spacing and utilize smaller time steps than the parent model. The function of the child model is to simulate phenomena that require a finer grid than the parent model contains, such as sharp changes in hydraulic gradient or abrupt changes in hydraulic properties that would otherwise be smeared by representation on the parent grid. The role of down-scaling from parent to child is to provide boundary conditions to the child model that are consistent with the regional flow

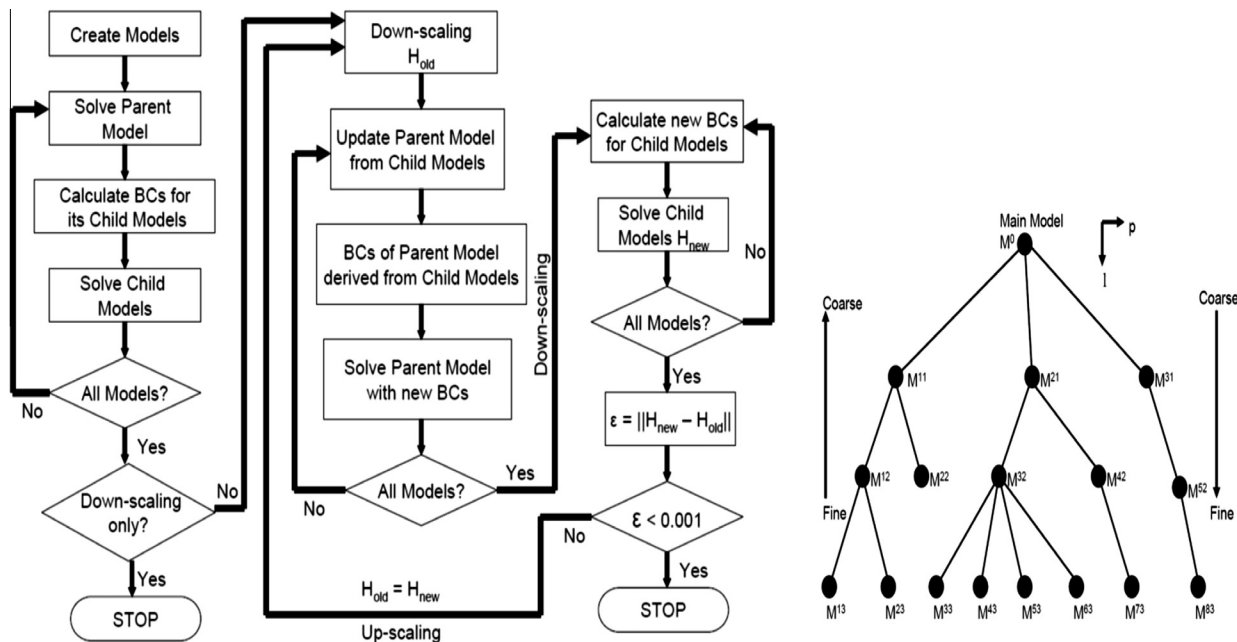


Fig. A.1. Flow chart of the up-scaling and down-scaling procedures utilized in HPDP (left), with a schematic of the hierarchical modeling structure (right).

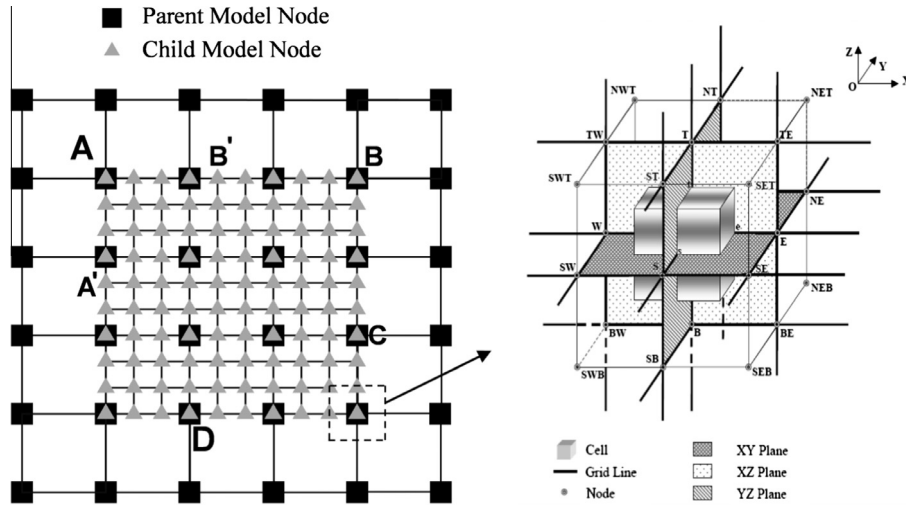


Fig. A.2. Typical cell and node configuration utilized in HPDP.

system, while up-scaling from child to parent model provides a feedback to the parent model such that the parent model's aggregated features are consistent with the details resolved in the child models. The coupling between the two grids occurs via boundary conditions at the interface between the parent model and its child models.

Boundary conditions along the interfaces of parent–child models can be in the form of prescribed head (Type 1) or prescribed flux (Type 2) as mentioned in Eq. (A.1). Therefore, combinations of boundary conditions in the parent–child models could be one of the following: (1) prescribed head in parent model and prescribed head in child model (H-H), (2) prescribed head in parent model and prescribed flux in child model (H-F), (3) prescribed flux in parent model and prescribed head in child model (F-H), or (4) prescribed flux in parent model and prescribed flux in child model (F-F). The approaches used to obtain head or flux boundary conditions in parent model from child model or vice versa are briefly described in the following paragraphs.

A.4.1. Down-scaling – specified-head boundary conditions for child model

To define the specified head boundary conditions along the interface of the child model, head values at the interface are derived from the parent model. As shown in Fig. A.3a, the head distribution in the parent model is known before down-scaling to the child model starts (i.e., heads at square nodes in Fig. A.3a are known, denoted as H_p). Along the parent–child model interface, some nodes are shared by both models. For these nodes, heads from the parent model apply directly to the child model, that is, $H_c = H_p$. For those child model nodes on the interface that do not share their location with a parent node, values of head need to be interpolated using the values at the shared nodes. If the child grid size is an integer divisor of that of the parent model ($n = \Delta X_p / \Delta X_c$), for example, $n = 2$ as shown in Fig. A.3a, then head values at the non-shared nodes can be easily calculated by using a linear interpolation scheme:

$$H_j = \frac{j}{n} H_{i+1} + \left(1 - \frac{j}{n}\right) H_i \quad (j = 1, \dots, n - 1) \quad (A.4)$$

where H_j is the unknown head at the j th non-shared node between H_i and H_{i+1} , which are the known heads at the i th and $(i + 1)$ th shared nodes, respectively.

A.4.2. Up-scaling – specified-head boundary conditions for parent model

The process of up-scaling is applied only after all of the solution has been obtained in the child model at the last model level L . Under the grid layout scheme using shared-nodes, if head values in the child model are known, head values at the parent model's grid nodes, denoted by squares in Fig. A.3b, can be very easily calculated as: $H_p = H_c$. Note that the process of up-scaling is not limited to only the nodes along the interface of the parent and child models, but also includes all the nodes in the entire child model domain that are shared by the parent model.

A.4.3. Down-scaling – specified-flux boundary conditions for child model

Flux in our hierarchical modeling system refers to the flux across the interface between the parent and child models. Defining specified flux boundary conditions for child models is a process of allocating fluxes from parent model cells to child model cells. To derive the specified flux boundary condition along the parent–grid interface, a flux balance on the interface is utilized (i.e., the net flow across the interfacing boundary from the parent model side equals that from the child model side).

Given the head values in the parent model, flux across the parent grid face AB from Fig. A.3c can be expressed in the following form:

$$Q_p \approx -K_n B \frac{H_N - H_S}{\delta_{NS}} \Delta X_p \quad (A.5)$$

where δ_{NS} is the distance between node N and node S in the parent model. In order to maintain a mass balance on the grid face AB , Q_p should be distributed among those child model cell-faces that are shared with AB . The simplest way to allocate Q_p to the child cell-faces is to distribute it in an area-weighted fashion, which can be written as

$$q_i = \frac{A_i}{\sum_{j=1}^{N_f} A_j} Q_p \quad (i = 1, \dots, N_f) \quad (A.6)$$

where q_i is the flux across the i th cell face that is shared with parent grid face AB , which has an area of A_i , and N_f is the total number of cell faces that are shared with parent grid face AB .

A.4.4. Up-scaling – specified-flux boundary conditions for parent model

As noted previously and seen clearly from the flux boundary calculations for the child model, defining specified flux boundary

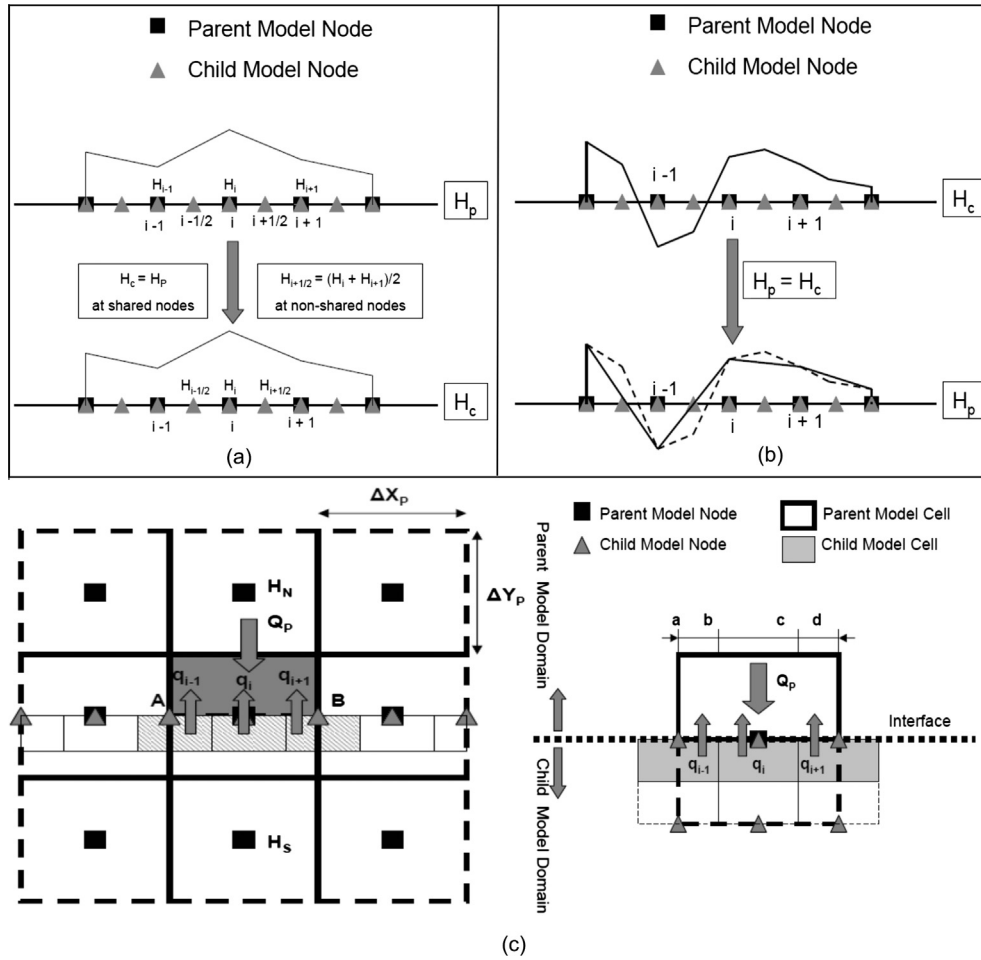


Fig. A.3. Schematics of the various up- and down-scaling algorithms used in HPDP. (a) Down-scaling using specified head boundary conditions; (b) up-scaling using specified head boundary; (c) up- and down-scaling using specified flux boundary conditions.

condition for the parent model is a process of balancing fluxes. Fig. A.3c shows a typical parent model cell represented by a dotted pattern and its three bordering child model cells represented by darker, patterned shading with indices of $i - 1$, i and $i + 1$. From Fig. A.3c, the net flow going into the parent cell is equal to the sum of the fluxes going out of the child model cells q_{i-1} , q_i and q_{i+1} ; that is,

$$Q_P = -(q_{i-1} + q_i + q_{i+1}) \tag{A.7}$$

where q_{i-1} or q_{i+1} represent the flux across the half cell-face of the child model, q_i represents the flux across a full cell-face of the child model, which are functions of the unknown head at nodes.

A.5. Solving matrix equations and iterative procedures

Application of Eq. (A.2) to each cell in the flow domain, and using the BCs as described above, results in a system of linear equations in the form of a septem-diagonal matrix:

$$[A]\{h\} = \{S_r\} \tag{A.8}$$

where $[A]$ is a square symmetric positive definite matrix consisting of the coefficients A_P , A_E , A_W , A_N , A_S , A_T and A_B from Eq. (A.3), $\{h\}$ is a vector consisting of the unknown hydraulic head values for current time step, and $\{S_r\}$ is the forcing vector consisting of known values from the previous time step and given fluxes. The linear system of equations (Eq. (A.8)) is then solved using a matrix solver.

There are five nested iterative procedures executed during each time step in our hierarchical modeling system. Innermost among these is the matrix solver to solve the system of equations subject to the FVM scheme; the second nested solver is for the head dependent source/sink terms; nonlinear unconfined head determination forms the intermediate iteration level; the coupling iteration of surface water and groundwater is embedded as the fourth iteration level and the down- and up-scaling loop is the outermost iteration level of the system. Once the convergence criterion for the outermost iteration is satisfied, the hierarchical modeling system moves to the next time step (in case of transient or flow simulations) or comes to a stop (for steady state simulations).

References

Anderson, M.P., Woessner, W.W., 1992. *Applied Groundwater Modeling*. Academic Press, San Diego.
 Afshari, S., Mandel, R., Li, S.G., 2008. Hierarchical patch dynamics modeling of near-well dynamics in complex regional groundwater systems. *J. Hydrol. Eng.* 13 (9), 894–904.
 Buxton, H.S., Reilly, T.E., 1986. A technique for analysis of ground-water systems at regional and subregional scales applied on Long Island, New York: Selected Papers in Hydrologic Science: U.S. Geological Survey Water-Supply Paper 2310, 129–142.
 Efendiev, Y., Durlafsky, L.J., Lee, S.H., 2000. Modeling of subgrid effects in coarse-scale simulations of transport in heterogeneous porous media. *Water Resour. Res.* 36 (8). <http://dx.doi.org/10.1029/2000WR900141>. issn: 0043-1397.
 Fung, L.S.-K., 1992. An Analysis of the Control-Volume Finite-Element Method for Flexible-Grid Reservoir Simulation, paper presented at the 1992 IBM Europe Summer Inst. Computational Methods and Tools in Reservoir Modeling, Oberlech, August 17–21.

- Gable, C.W., Trease, H.E., Cherry, T.A., 1996. Geological applications of automatic grid generation tools for finite elements applied to porous flow modeling. In: Soni, B., Thompson, J., Eiseman, P., Hauser, J. (Eds.). Proceedings of the 5th International Conference on Numerical Grid Generation in Computational Fluid Dynamics and Related Fields, Mississippi State University, April 1996, ERC-MSU Press.
- Heinemann, Z.E., Gerken, G., von Hantelmann, G., 1983. Using local grid refinement in a multiple-application reservoir simulator. In: SPE Reservoir Simulation Symposium, 15–18 November 1983, San Francisco, California.
- Hill, M.C., Tiedeman, R.C., 2007. *Effective Groundwater Model Calibration – with Analysis of Data, Sensitivities, Predictions, and Uncertainty*. John Wiley & Sons Inc., Hoboken, New Jersey.
- Li, S.G., Liu, Q., 2006. Software News – “Interactive Ground Water (IGW)”, *Environmental Modeling and Software*, vol. 21(3).
- Li, S.G., Liu, Q., 2006b. A real-time, interactive steering environment for integrated ground water modeling. *J. Groundwater* 44, 758–763.
- Li, S.-G., Liu, Q., 2008. A new paradigm for groundwater modeling. In: Cai, X., Yeh, J. (Eds.), *Quantitative Information Fusion for Hydrological Sciences*, p. 19–41.
- Li, S.G., Liu, Q., Afshari, S., 2006. An object-oriented hierarchical patch dynamics paradigm (HPDP) for groundwater modeling. *Environ. Model. Software* 21 (5), 744–749.
- Li, S.G., Liao, H., Afshari, S., Oztan, M., Abbas, H., Mandel, R., 2009. A GIS-enabled hierarchical patch dynamics paradigm for modelling complex groundwater systems across multiple spatial scales. In: *Modeling Pollutants in Complex Environments*, vol. 1, Hanrahan, Grady, St. Albans, UK, ILM Publications, p. 177–216.
- Liao, H.S., Sampath, P.V., Curtis, Z.K., Li, S.G., 2015. Hierarchical modeling and parameter estimation for a coupled groundwater-lake system. *J. Hydro. Eng.*, 04015027.
- Matott, L.S., Rabideau, A.J., Craig, J.R., 2006. Pump-and-treat optimization using analytic element method flow models. *Adv. Water Resour.* 29 (5), 760–775.
- Mehl, S., Hill, M.C., 2002. Development and evaluation of a local grid refinement method for block-centered finite-difference groundwater models using shared nodes. *Adv. Water Resour.* 25, 497–511.
- National Weather Service, National Oceanic and Atmospheric Administration. U.S. Dept. of Commerce. <<http://www.nws.noaa.gov/>> (accessed 12.02.15).
- Peaceman, D.W., 1978. Interpretation of well-block pressures in numerical reservoir simulation. *SPE J.* 253, 183–194.
- Prickett, T.A., 1967. Designing pumped well characteristics into electrical analog models. *Groundwater* 5 (4), 38–46.
- Pritchett, J.W., Garg, S.K., 1980. Determination of effective well block radii for numerical reservoir simulations. *Water Resour. Res.* 16 (4), 665–674. <http://dx.doi.org/10.1029/WR016i004p00665>.
- Sutradhar, A., Paulino, G.H., 2004. A simple boundary element method for problems of potential in non-homogeneous media. *Int. J. Numer. Meth. Eng.* 60 (13), 2203–2230.
- Theis, C.V., 1935. The relation between the lowering of the piezometric surface and the rate and duration of discharge of a well using groundwater storage. *Trans. Am. Geophys. Union* 2, 519–524.
- Thiem, G., 1906. *Hydrologische methoden* (in German). In: Gebhardt, J.M. (Ed.), *Hydrologic Methods*, Leipzig, Germany, pp. 56.
- Townley, L.R., Wilson, J.L., 1980. Description of and user's Manual for a Finite-Element Aquifer flow Model AQUIFEM-1. Cambridge, Massachusetts: Ralph M. Parson Laboratory Technology Adaption Program.
- Trescott, P.C., Pinder, G.F., Larson, S.P., 1976. *Finite-Difference Model for Aquifer Simulation in two Dimensions with Results of Numerical Experiments*. U.S. Geological Survey, Chap. C1, Bk.7.
- Ward, D.S., Buss, D.R., Mercer, J.W., Hughes, S.S., 1987. Evaluation of a groundwater corrective action at the Chem-Dyne hazardous-waste site using a telescopic mesh refinement modeling approach. *Water Resour. Res.* 23, 603–617.